GLOBAL PATTERN OF MESOSCALE VARIABILITY IN SEA SURFACE HEIGHT AND ITS DYNAMICAL CAUSES

Alexey Kaplan, alexeyk@ldeo.columbia.edu
Mark A. Cane, mcane@ldeo.columbia.edu
Dake Chen, dchen@ldeo.columbia.edu

Climate Modeling Group, Division of Ocean and Climate Physics
Lamont-Doherty Earth Observatory of Columbia University, Palisades, NY 10964, United States

1. INTRODUCTION

Using gridded satellite altimetry fields, we separate the mesoscale variability of sea surface heights into its spatial and temporal components. The ratio of these components shows a strong latitudinal dependence and to a large degree is controlled by Rossby radius of deformation for the first baroclinic mode. Further analysis results in the attribution of mesoscale variability in different areas to dynamical causes. Major portion of it can be explained as a local response to the mesoscale variability in the wind. The propagation of ocean eddies modify the pattern in such areas and nearby. Another major mechanism of generating high mesoscale variability is generation of instability waves in the areas of ocean countercurrents. Comparison with ocean models show that they mostly reproduce mesoscale variability due to current instabilities, but not the one caused by the mesoscale variability in winds. Eddy-permitting ocean models reproduce temporal variability much better than the spatial variability, although the simulation of the latter is improved with the refinement of models' resolution. The pattern of mesoscale variability often appears as a pattern of model error and also as a pattern of gridding error on altimetry-based sea surface height maps.

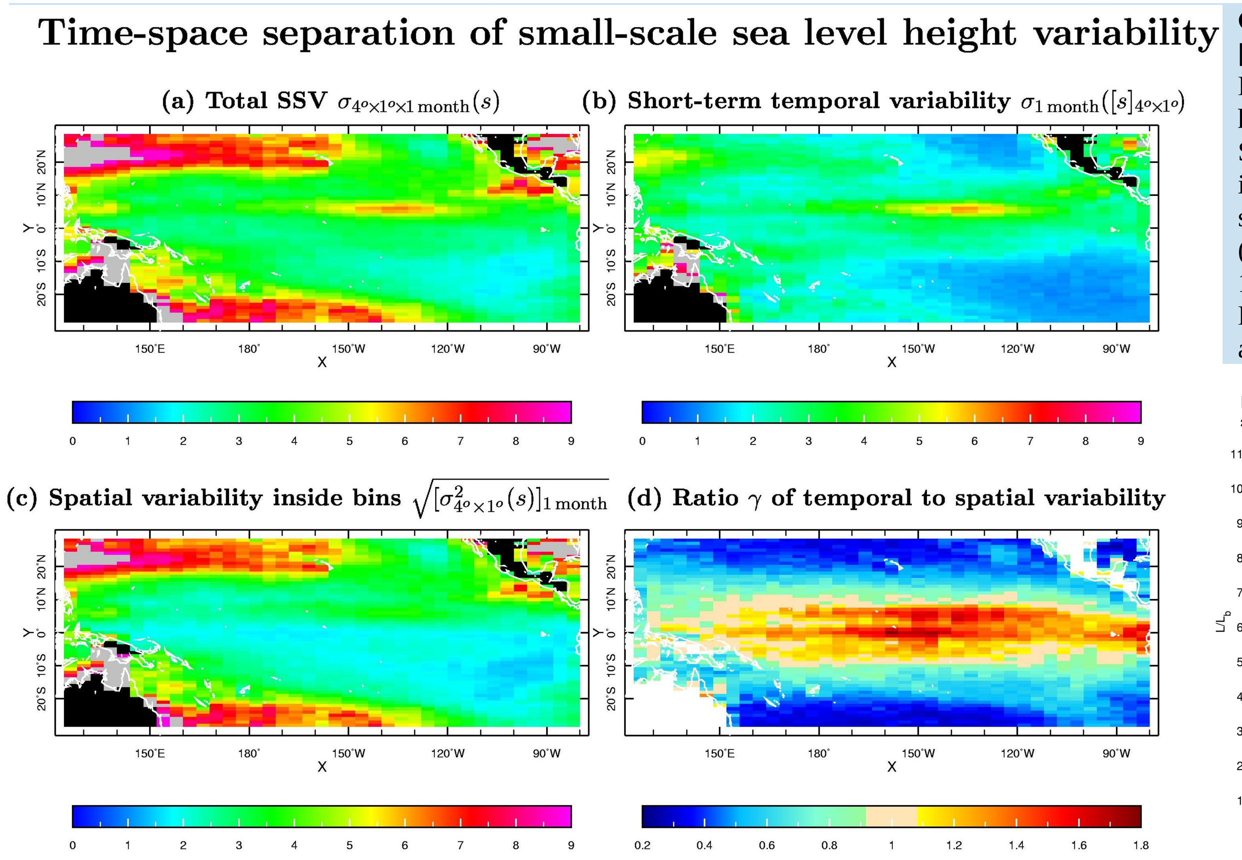

On the left: Separation of space-time sea level height SSV into temporal and spatial components for Ducet et al. [2000] 0.25 degree resolution 10 day gridded altimetry fields.
Below left: Ratios of temporal to spatial variability for ocean waves. Colors show the ratio for a monochromatic harmonic wave with a wavelength L and a period T. White lines show dispersion relations for ocean waves. Solid lines indicate Rossby (R) waves. Thin lines show off-equatorial Rossby waves for different latitudes indicated at black circles that mark points with the minimum allowable wave period for each latitude. Thick lines show the first 3 trapped equatorial Rossby modes. Dashes and dash-points show equatorial Kelvin (K) and Yanai (Y) waves respectively. White dots indicate Poisson (P) waves for the latitudes of 5 and 29 degree. Box scales of 1 month and 4 degree are used.
Below right: Zonal averages for the ratio of temporal to spatial variability estimated from the Ducet et al. [2000] analyzed altimetry fields (thick solid line) and the theoretical estimates (marked lines).

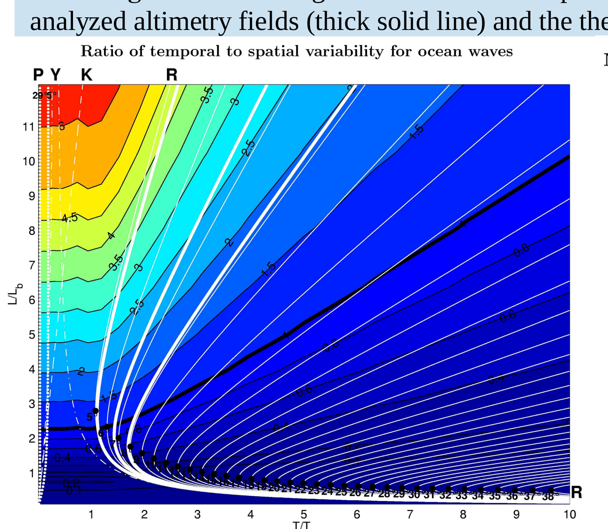

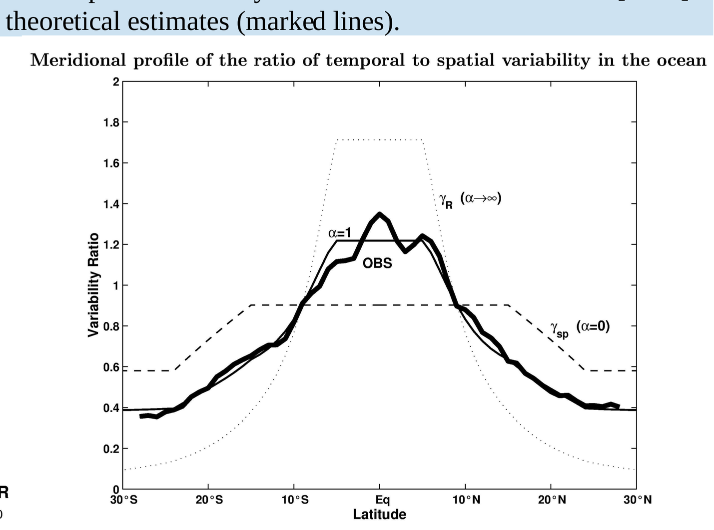

Monte Carlo experiments with a linear model

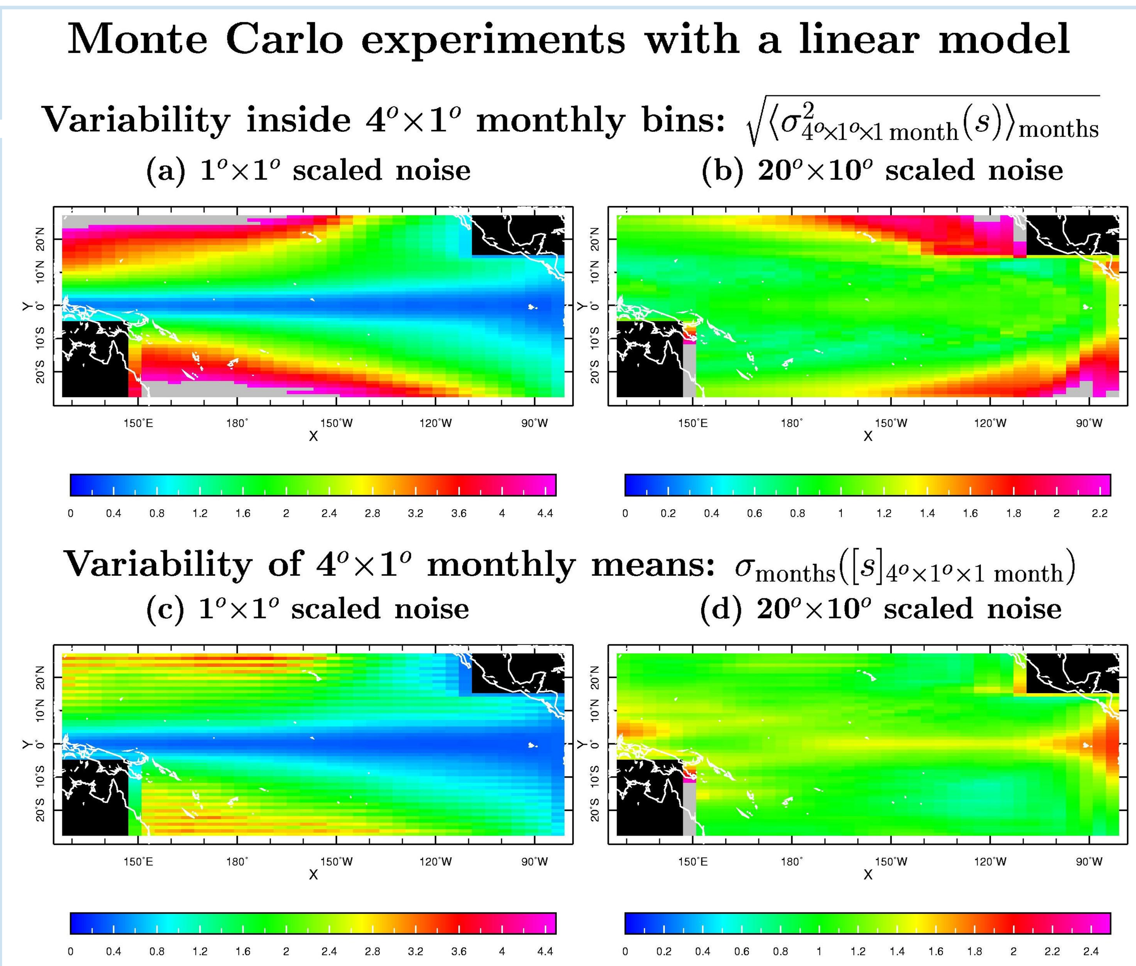

Small-scale variability in wind and sea level height

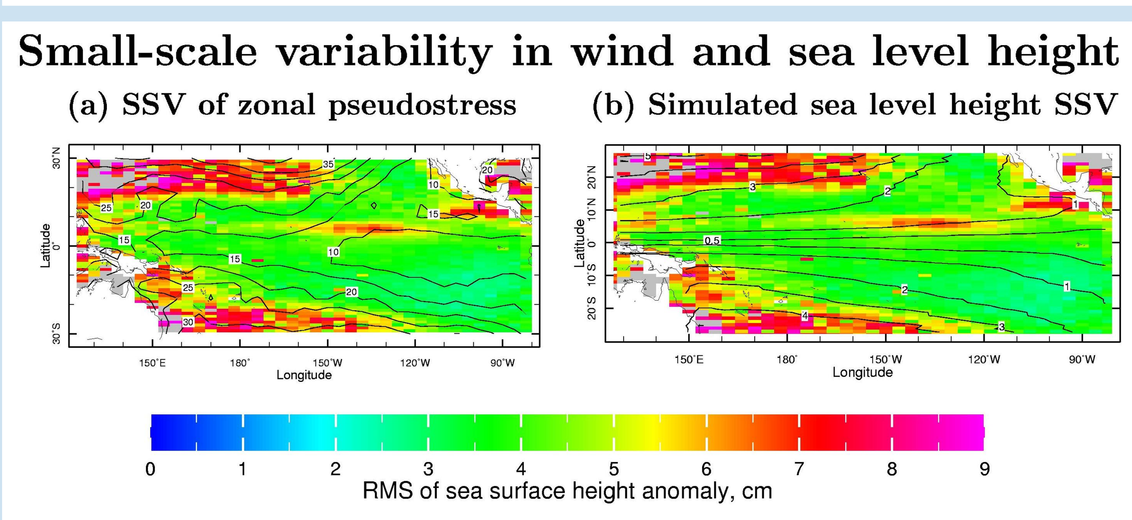

High above: Simulation of sea level height error and SSV in Monte Carlo experiments with a linear model forced by noise designed to imitate errors in the wind forcing. Shown are model responses to the noise forcings with short (1 degree) and relatively long (20 degree zonal and 10 degree meridional) spatial decorrelation scales. **Above**:Temporal decorrelation scale is 0.25 month. SSV in pseudostress and sea level height response: Contours of SSV RMS in zonal wind pseudostress, (m/s)**2, are shown over the color pattern of SSV, and same but for contours of the SSV RMS in the sea level height response of a linear model to the random wind with 1 degree spatial and 0.25 month temporal decor-relation scales. **Below:** A contrast between ROMS NPac SSH RMS with satellite altimetry (Curchitser et al, 2005) and SSH response to AMIP-based surface flux perturbations (Borovikov et al. 2005).

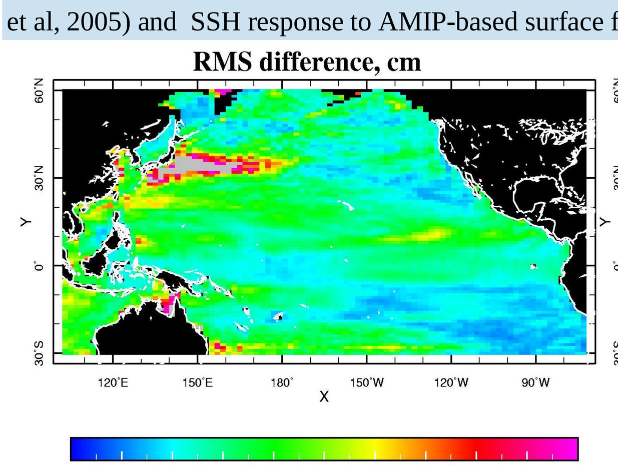

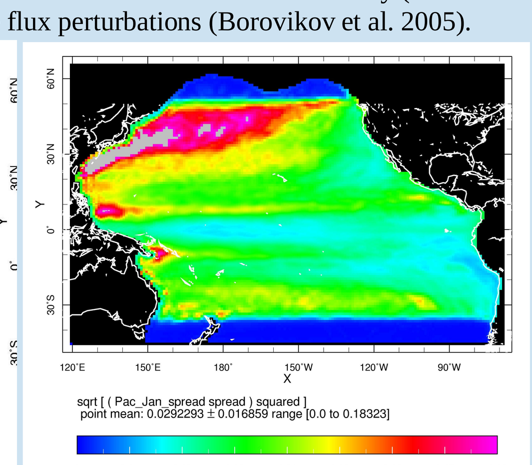

TOPEX [*Ducet et al.* 2000]

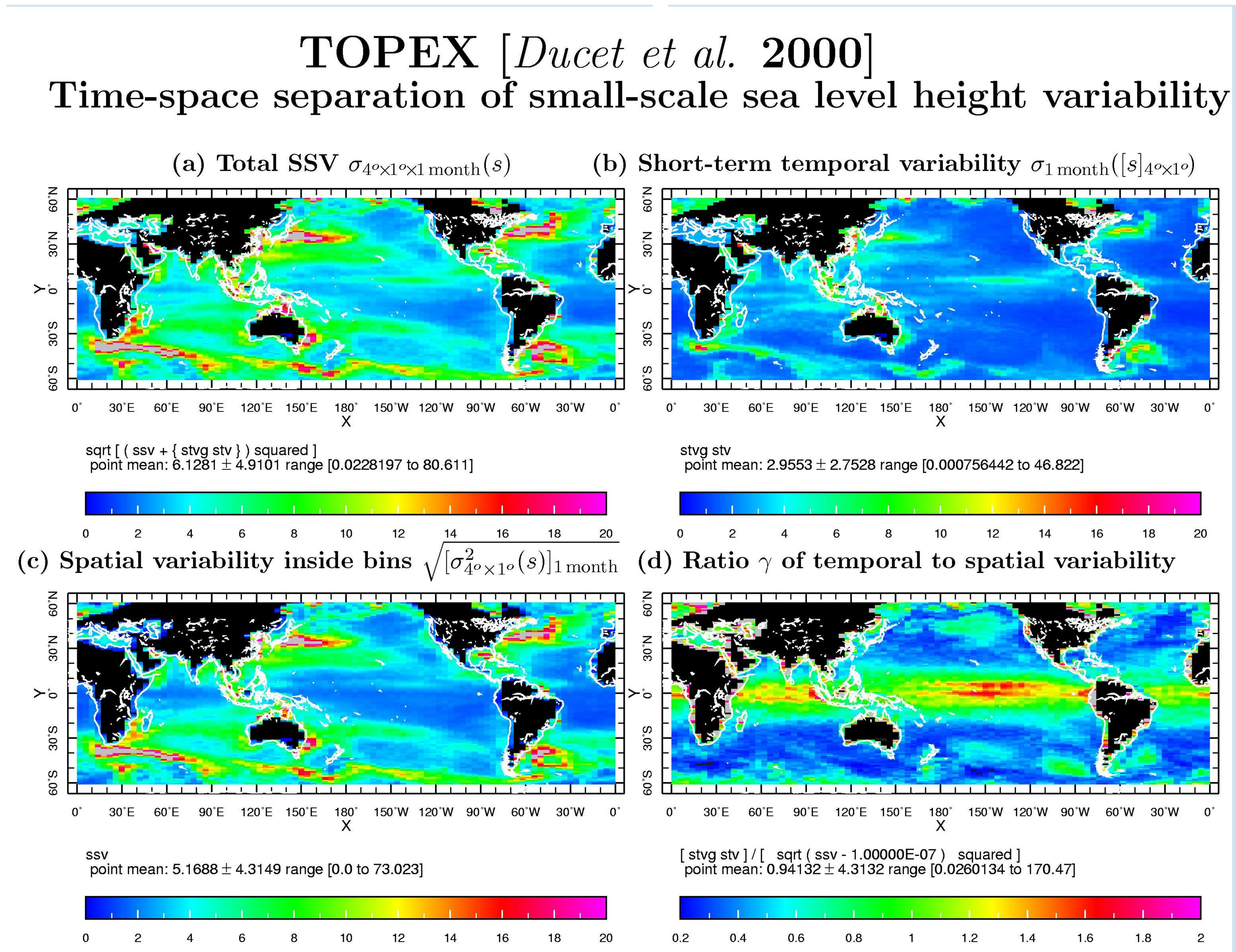

POCM 4C model [*Tokmakian and Challenor* 1999]

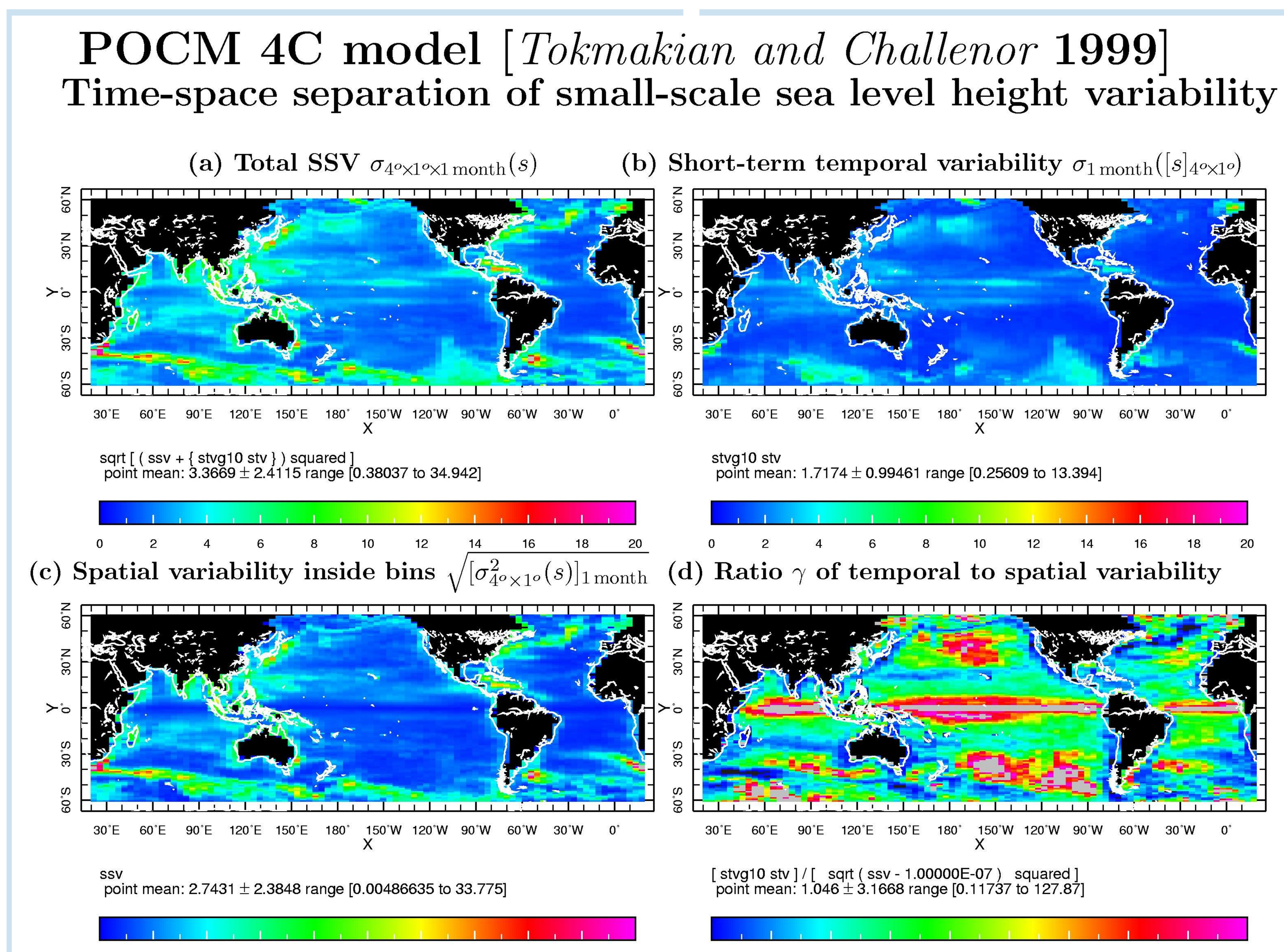

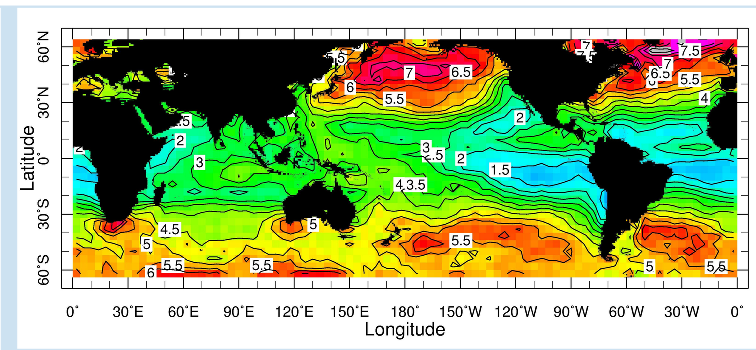

Left above: Separation of the global field of altimetry-based sea surface height SSV into spatial and temporal components.

Left below: Same but for the POCM 4C model.

Above: Small-scale variability in the surface winds (from satellite scatterometry).

Below: Contours of the surface wind SSV are shown over color plots of the total SSH SSV and their model-to-altimetry ratios.

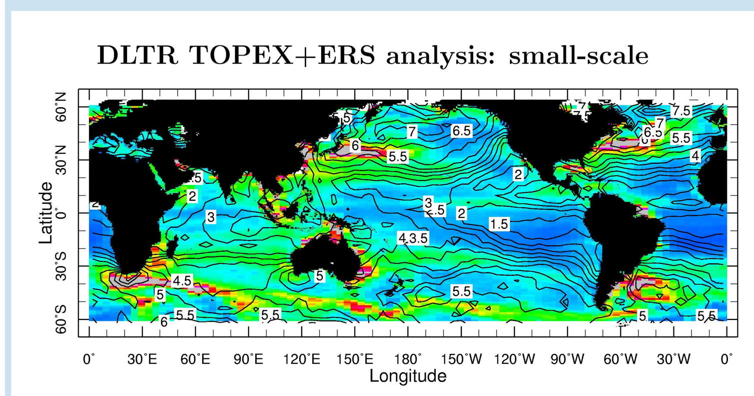

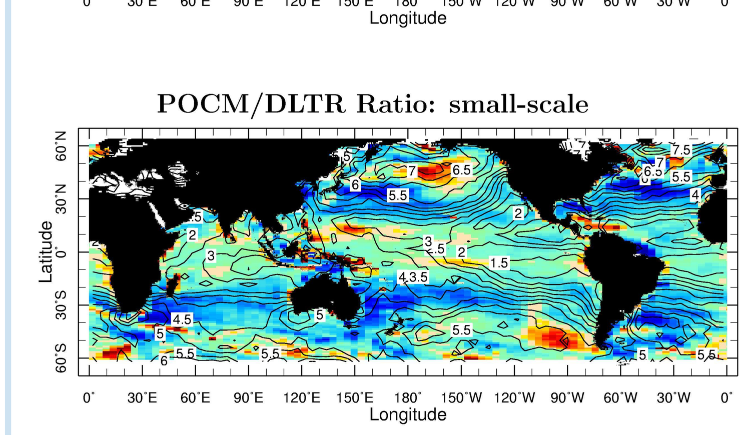

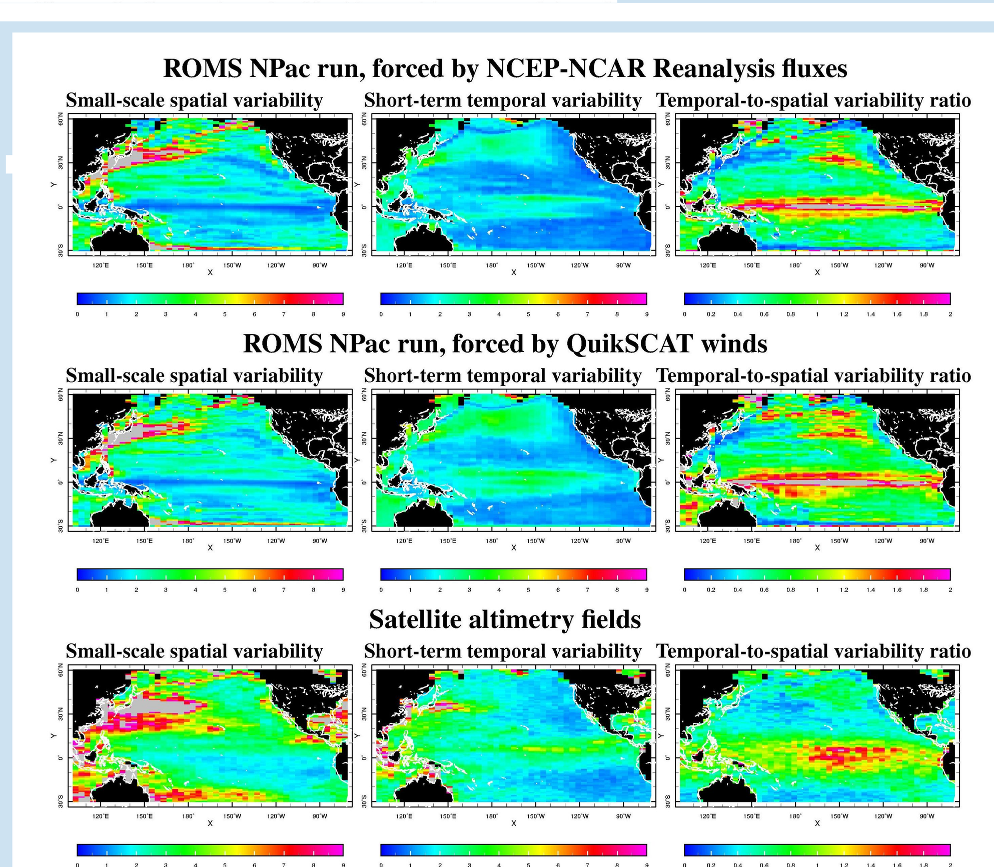

On the left: Small-scale spatial variability inside 4 degree by 1 degree boxes, temporal variability (standard deviations of these box means computed within 1 month intervals, and their ratios. Shown are ROMS NPac run forced by Reanalysis fluxes and by QuikSCAT winds (Curchitser et al. 2005) and Ducet et al. (2000) blended analyses of Topex/Poseydon and ERS-1,2 satellite altimetry. All statistics are averaged for for the QuikSCAT run period of 2000-2002.

On the right: Same as on the left but constrained to the area and period (year 2000) of California Coastal Current System ROMS simulation (Powell et al. 2006), which is also shown.

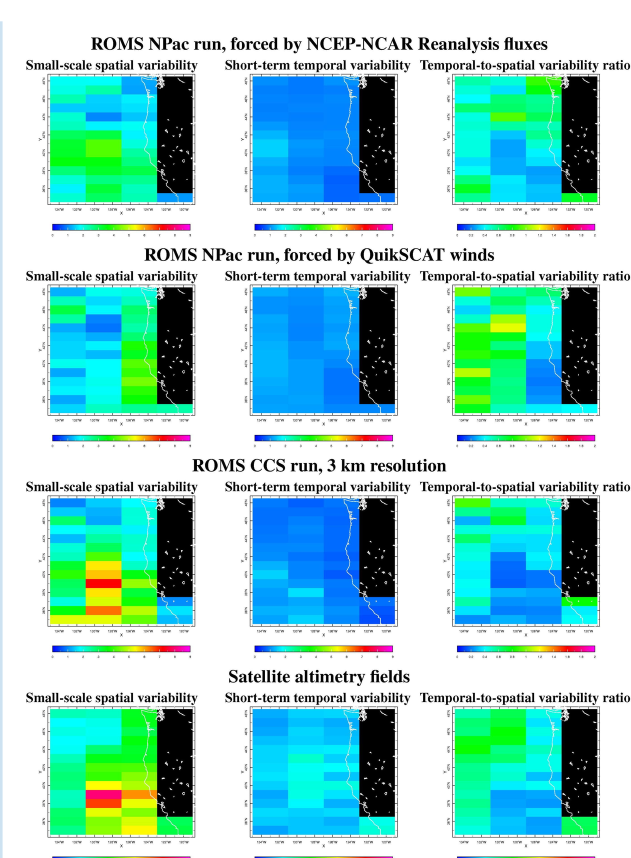

REFERENCES

Borovikov A, Rienecker MM, Keppenne CL, Johnson GC, 2005: Multivariate error covariance estimates by Monte Carlo simulation for assimilation studies in the Pacific Ocean. *Monthly Weather Review,* **133**, 2310-2334.

Curchitser, E.N., D.B. Haidvogel, A.J. Hermann, E.L. Dobbins, T.M.Powell, and A.Kaplan, 2005: Multi-scale modeling of the North Pacific Ocean: Assessment and analysis of simulated basin-scale variability (1996-2003), *J. Geophysical Res.*, **110**, C11021, doi10.1029/2005JC002902.

Ducet, N., P.-Y. Le Traon, and G. Reverdin, 2000: Global high-resolution mapping of ocean circulation from TOPEX/Poseidon and ERS-1 and -2. *J. Geophys. Res*., **105**, 19,477-19,498.

Kaplan, A., M.A. Cane, D. Chen, D.L. Witter, R.E. Cheney, 2004: Small-scale variability and model error in tropical Pacific sea level. *J. Geophysical Res.*, **109**, C02001, doi:10.1029/2002JC001743.

Powell, T. M., C.V.W. Lewis, E.N. Curchitser, D.B. Haidvogel, A. Hermann, E. Dobbin, 2006: Results from a three-dimensional, nested biological-physical model of the California Current System and comparisons with statistics from satellite imagery, *J. Geophys. Res*., **111**, C07018, doi:10.1029/2004JC002506.

Acknowledgements: This work was supported by the NASA Ocean Surface Topography Science Team, ONR AESOP and Joint Center for Satellite Data Assimilation grants to Lamont-Doherty Earth Observatory of Columbia University.